Published in final edited form as:
Acta Biomater. 2012 March ; 8(3): 978–987. doi:10.1016/j.actbio.2011.11.031.

Macrophage Phenotype as a Predictor of Constructive Remodeling following the Implantation of Biologically Derived Surgical Mesh Materials

Bryan N. Brown[1], **Ricardo Londono**[1], **Stephen Tottey**[1], **Li Zhang**[1], **Kathryn A. Kukla**[1], **Matthew T. Wolf**[1], **Kerry A. Daly**[1], **Janet E. Reing**[1], and **Stephen F. Badylak**[1,*]

Bryan N. Brown: brown@cornell.edu; Ricardo Londono: rlondo@gmail.com; Stephen Tottey: totteys@upmc.edu; Li Zhang: zhangl2@upmc.edu; Kathryn A. Kukla: kkukla@andrew.cmu.edu; Matthew T. Wolf: wolf.matthew.t@gmail.com; Kerry A. Daly: dalykerrya@gmail.com; Janet E. Reing: reinjx@upmc.edu; Stephen F. Badylak: badylaks@upmc.edu

[1]McGowan Institute for Regenerative Medicine, University of Pittsburgh, Suite 300, 450 Technology Drive, Pittsburgh, PA 15219

Abstract

Macrophages have been classified as having plastic phenotypes which exist within a spectrum between M1 (classically activated; pro-inflammatory) and M2 (alternatively activated; regulatory, homeostatic). To date, the effects of polarization towards a predominantly M1 or M2 phenotype have been studied largely in the context of response to pathogen or cancer. Recently, M1 and M2 macrophages have been shown to play distinct roles in tissue remodeling following injury. In the present study, the M1/M2 paradigm was utilized to examine the role of macrophages in the remodeling process following implantation of 14 biologically derived surgical mesh materials in the rat abdominal wall. In situ polarization of macrophages responding to the materials was examined and correlated to a quantitative measure of the observed tissue remodeling response to determine whether macrophage polarization is an accurate predictor of the ability of a biologic scaffold to promote constructive tissue remodeling. Additionally the ability of M1 and M2 macrophages to differentially recruit progenitor-like cells in vitro, which are commonly observed to participate in the remodeling of those ECM scaffolds which have a positive clinical outcome, was examined as a possible mechanism underlying the differences in the observed remodeling responses. The results of the present study show that there is a strong correlation between the early macrophage response to implanted materials and the outcome of tissue remodeling. Increased numbers of M2 macrophages and higher ratios of M2:M1 macrophages within the site of remodeling at 14 days were associated with more positive remodeling outcomes ($r^2=0.525–0.686$, $p<0.05$). Further, the results of the present study suggest that the constructive remodeling outcome may be due to the recruitment and survival of different cell populations to the sites of remodeling associated with materials that elicit an M1 versus M2 response. Both M2 and M0 macrophage conditioned medias were shown to have higher chemotactic activities than media conditioned by

Corresponding Author: Stephen F. Badylak, Suite 300, 450 Technology Drive, Pittsburgh, PA 15219, Tel: (412) 235-5253, Fax: (412) 235-5256, badysx@upmc.edu.

M1 macrophages ($p<0.05$). A more thorough understanding of these issues will logically influence the design of next generation biomaterials and the development of regenerative medicine strategies for the formation of functional host tissues.

2.0 Introduction

Biologic materials composed of extracellular matrix (ECM) have been harvested from a wide variety of tissues and organs and have been used in a similarly wide variety of preclinical and clinical applications [1, 2]. It has been shown that ECM based materials, if prepared and utilized appropriately, are capable of acting as inductive templates for the formation of site-specific functional host tissues following implantation [3–5]. Alternatively, if processing methods do not effectively decellularize the source tissue, involve chemicals that create non-degradable molecular cross-links, or leave residual reagents in the ECM, then the in-vivo remodeling response is less desirable and characterized by chronic inflammation, fibrotic encapsulation, and scar tissue formation [6–8]. The mechanisms by which biologic mesh materials elicit either “constructive remodeling” or chronic inflammation, however, are only partially understood.

The process of tissue remodeling following implantation has been shown to be invariably associated with a robust macrophage response beginning as early as two days post-implantation and continuing for several months depending on the mesh material and the clinical application in which it is used [8]. The prolonged presence of macrophages at a site in which the remodeling outcome can range from scarring to healthy functional tissue formation suggests a central, and perhaps determinant, role for macrophages in tissue remodeling following surgical mesh implantation.

Activated macrophages possess diverse, plastic phenotypes that play an important role in the host inflammatory response and the process of tissue repair and remodeling following injury [9–14]. Macrophage phenotype is dependent upon interactions with microbial and non-microbial components as well as the cytokines and chemokines secreted by other cells within the microenvironment [10, 15, 16]. Macrophage phenotype has been broadly characterized as M1, or “classically” activated, and M2, or “alternatively” activated, mimicking the Th1/Th2 nomenclature [15]; however, it is well recognized that macrophages are a heterogeneous cell population and that M1 and M2 represent extremes on a spectrum of macrophage phenotypes [9, 10, 16]. M1 refers to macrophages activated by bacterial lipopolysaccharide (LPS) and interferon-γ (IFN-γ) and possessing characteristics which include production of large amounts of pro-inflammatory signaling and effector molecules, efficient antigen presentation, killing of intracellular pathogens, tumor destruction, and promotion of polarized Th1 responses. M2 refers to macrophages which are activated by interleukin (IL)-4, IL-10, IL-13, or a combination thereof, and possessing immunoregulatory or tissue remodeling characteristics which include minimal production of pro-inflammatory molecules, expression of scavenger, mannose, and galactose receptors, increased phagocytic activity, and participation in polarized Th2 reactions. M2 macrophages have been further shown to consist of subdivisions including M2a, M2b, and M2c depending on the activating signals and functional characteristics [10]. The exact role of each M2 subtype in tissue remodeling is not well defined. However, heterogeneity and plasticity of macrophage

phenotype are increasingly recognized as playing an important role in the response to pathogens and tissue injury as well as in the development and progression of a variety of diseases including obesity, atherosclerosis, and cancer [17–19].

The macrophage population present immediately following tissue injury possesses predominantly M1 characteristics [20, 21]. Transition to an M2 phenotype occurs concurrently with resolution of the inflammatory process and the initiation of the remodeling phase of wound healing [20]. This process represents the default mammalian host response to tissue injury, and generally results in the formation of localized scar tissue. Certain biologic mesh materials have been shown to modulate this default host response and facilitate the formation of site-appropriate functional host tissue instead of scar tissue [6, 7]. Recent work shows that the presence of distinct phenotypic populations of macrophages at early time points following implantation may be predictive of downstream outcomes consistent with constructive tissue remodeling [6, 7].

The present study examined both the in vivo host remodeling response to 14 FDA approved, biologically derived surgical mesh materials and the in vitro chemotactic response of a muscle progenitor cell type toward the secreted products of phenotypically distinct macrophages. The mesh materials were all composed of naturally occurring biomaterials but varied in their tissue and species source and method of production. The in situ polarization of macrophages following device implantation was determined and correlated to the observed real time and downstream tissue remodeling outcomes. The in vitro chemotactic studies were conducted to examine a potential mechanism by which lineage directed cells participate in constructive, site specific remodeling.

3.0 Methods

3.1 Test Articles

The biologic mesh materials evaluated, their manufacturer, and composition are listed in Table 1. All materials were received sterile and trimmed to size (1 cm x 1 cm) prior to implantation. It should be noted that all of the devices examined in the present study were commercially available materials in their original packaging. Therefore, while not quantitatively measured in the present study, all materials were assumed to meet FDA mandated standards for endotoxin content (<20 EU/mL).

3.2 Animal Model

Fifty six Sprague-Dawley rats were randomly divided into fourteen separate groups of four each. Each rat was subjected to the surgical procedure described below and one of the mesh materials listed in Table 1 was implanted in each animal. The treatment groups were then subdivided into two groups of two each that were sacrificed and explanted at 14 or 35 days post-surgery (n=2 for each test article at each time point).

A previously described abdominal wall defect model was used [8, 22]. Each rat was anesthetized and maintained at a surgical plane of anesthesia with 2% isoflurane in oxygen. The surgical site was prepared in sterile fashion using a betadine (providone-iodine) solution followed by placement of sterile drapes. A ventral midline incision was made and the

adjacent subcutis bluntly dissected to expose the ventral lateral abdominal wall including the musculotendinous junction of the oblique musculature.

Defects measuring 1 cm x 1 cm were created in the exposed musculature (external and internal oblique muscles), leaving the underlying peritoneum and transversalus fascia and the overlying skin intact. The defects were then repaired with one of the mesh materials listed in Table 1. Each implant was sutured to the adjacent abdominal wall with 4-0 Prolene non-absorbable suture at each corner to secure the mesh, to allow for partial mechanical loading of the test article, and to allow for identification of the implant boundaries at the time of euthanasia and explanation. A minimal amount of suture material was used to avoid eliciting a host response to the suture material that would obscure the host response to the mesh material itself. The skin was closed using absorbable 4-0 Vicryl suture. The animals were recovered from anesthesia on a heating pad and allowed normal activity and diet for the remainder of the study period

Animals were euthanized at 14 or 35 days post-implantation and the implant sites including adjacent native tissue were explanted. All animal procedures were approved by the Institutional Animal Care and Use Committee at the University of Pittsburgh.

3.3 Histomorphologic Analysis

The explanted specimens were fixed in formalin and embedded in paraffin prior to being cut into 6 μm thick sections and mounted on glass slides. The specimens were deparaffinized with xylenes followed by exposure to a graded series of ethanol solutions (100-70%). Sections then were stained with hematoxylin and eosin and dehydrated using the reverse of the deparaffinization treatment described above prior to coverslipping.

Histologic sections were evaluated by two blinded investigators using previously validated [8] quantitative criteria for aspects of inflammatory and tissue remodeling response. Criteria included cellular infiltration, the presence of multinucleate giant cells, vascularity, connective tissue organization, encapsulation, test article degradation, and the presence of muscle cells within the site of implantation. All aspects were evaluated on a scale between 0 and 3 (Table 2). Higher scores were more indicative of a constructive remodeling response while low scores were more indicative of a scar tissue or foreign body type response. The suture sites were avoided in the morphologic evaluation. Different scoring criteria were used at 14 and 35 days, reflecting differences in acute and chronic inflammatory responses as well as in early and later phases of tissue remodeling. A list of the scoring criteria used to evaluate the histologic response at 14 and 35 days is provided in Supplemental Table 1. Scores from both investigators were averaged and scores from each category were added to form an aggregate score for each mesh.

3.5 Determination of Macrophage Phenotype by Immunolabeling

Immunolabeling was performed on 6 μm sections of the implant sites. Following deparaffinization, the slides were placed in citrate antigen retrieval buffer (10 mm citric acid monohydrate, pH 6.0) which was then brought to a boil (95–100 °C) for 20 min. The buffer was allowed to cool and the slides were then washed twice in TRIS buffered saline/Tween 20 (Trizma Base, Sigma; Tween 20, Sigma) solution (pH 7.4) and twice in PBS. The

sections were incubated in 2% normal horse serum, 1% BSA, 0.1% Triton X-100, and 0.1% Tween 20 in PBS (pH 7.4) for 1 h at room temperature in a humidified chamber to inhibit non-specific binding of the primary antibody. Following incubation in blocking serum, the sections were incubated in primary antibodies in a humidified chamber at 4 °C overnight. Each tissue specimen was exposed to antibodies to a pan-macrophage marker (CD68), an M1 macrophage phenotype marker (CCR7), and an M2 macrophage phenotype marker (CD206). Following the overnight incubation, the slides were washed three times in PBS prior to incubation in fluorescently labeled secondary antibodies for one hour in a humidified chamber at room temperature, and then subjected to three more washes in PBS. Slides were then exposed to a DRAQ5 nuclear stain for 30 minutes at 37°C prior to being washed three times in PBS. The slides were then coverslipped using aqueous mounting media prior to visualization under a fluorescent microscope. Each PBS rinse in the protocol was for 3 min at room temperature, with occasional agitation.

The primary antibodies used were mouse anti-CD68 (Serotec) at a dilution of 1:50, rabbit anti-CCR7 (Epitomics) at a dilution of 1:200, and goat anti-CD206 (Santa Cruz) at a dilution of 1:50. The secondary antibodies used were AlexaFluor donkey anti-mouse IgG (350 nm) at a dilution of 1:25, donkey anti-rabbit IgG (568 nm) at a dilution of 1:100 and donkey anti-goat IgG (488 nm) at a dilution of 1:100. All antibodies were diluted in blocking serum as described above.

The immunolabeled slides were examined and imaged by a blinded investigator using a Nikon e600 microscope equipped with a Nuance multi-spectral imaging system. Fluorescence images were then subjected to spectral unmixing and re-coloring for autofluorescence removal and quantitative analysis. The images were then evaluated in a blinded fashion by two separate independent investigators. Quantitative analysis was performed by selecting three areas of approximately 90 x 60 μm at the interface of the mesh and adjacent native tissue, and encompassing the 2–3 cell layers closest to the mesh surface from within a high power microscope field (40x magnification). The number of cells labeled positively for each marker within the three boxes was then counted and summed for each image. The mean of the sums for three high power images was then calculated for each sample. Counts of cells by both blinded investigators for those cells which expressed each individual marker were averaged. A ratio of the number of M2 (CD206+) cells to M1 (CCR7+) cells was also calculated for each field as follows:

$$M2{:}M1 = \frac{Number\ \ M2\ \ Cells}{Number\ \ M1\ \ Cells}$$

3.6 Evaluation of Chemotaxis Towards Macrophage Conditioned Media

3.6.1 RAW 264.7 Mouse Macrophage Culture and Macrophage Conditioned Media Production—

RAW 264.7 macrophages were cultivated in Dulbecco's minimal essential medium (DMEM) containing 10% fetal bovine serum and 1% penicillin/streptomycin. Cells were grown at 37°C in 5% CO_2/95% air, and were split when they were approximately 80% confluent. Macrophages were passaged once following thawing and then allowed to reach 80% confluence. Cells were then removed from the cell culture flask

using a rubber cell scraper and re-suspended at a concentration of 1 x 10^6 cells/mL of cell culture media.

Macrophages were then subjected to one of three well-described polarization protocols in a 6 well cell culture plate at a concentration of 2 x 10^6 cells/well (2 mL/well). M0 (un-polarized) macrophages were cultured in DMEM with 10% fetal bovine serum. M1 macrophages were cultured in DMEM with 10% fetal bovine serum supplemented with 20 ng/mL IFN-γ and 100 ng/mL LPS. M2 macrophages were cultured in DMEM with 10% fetal bovine serum supplemented with 20 ng/mL IL-4. Macrophages were cultured in polarization media for 24 hours post-plating. Following the 24 hour polarization period, the polarization media was aspirated from all wells and the cells were rinsed once using 37°C PBS and once using 37°C serum free DMEM to remove polarization media. Following rinsing, 2 mL of serum free DMEM was placed in each well and the polarized macrophages were allowed to condition the media for 4, 8, 12, and 24 hours. At each specified time point, the conditioned media was removed from each plate and stored at −80°C until use in the Boyden chamber chemotaxis assay described below.

3.6.2 C2C12 Myoblast Culture—C2C12 mouse myoblast-like cells were cultivated in DMEM containing 10% fetal bovine serum and 1% penicillin/streptomycin. Cells were grown at 37°C in 5% CO2/95% air, and were harvested for Boyden chamber analysis when they were approximately 80% confluent.

3.6.3 Boyden Chamber Assay—Migration of C2C12 myoblast-like cells towards macrophage-conditioned media was investigated using a Boyden chamber assay. C2C12 myoblasts were placed into starvation media (DMEM with 0.5% heat-inactivated fetal calf serum) in a 37°C in 5% CO2/95% air incubator for 16 hours prior to use in the Boyden chamber assay. Cells were then trypsinized and re-suspended in serum free media and incubated in a 50 mL conical tube for 1 hour in suspension in a humidified 95% air/5% CO2 incubator. Polycarbonate chemotaxis filters with a pore size of 8μm were coated with 0.05 mg/mL collagen type I. Macrophage conditioned medias (M0, M1, or M2) as well as positive (media + 10% fetal calf serum) and negative (serum free media) control medias were added to the lower wells of a Neuro Probe 48-well micro chemotaxis chamber. The collagen coated chemotaxis filter was then placed over the macrophage conditioned media and 50,000 cells were added to each of the upper wells of the chemotaxis chamber. Cells were then allowed to migrate across the chemotaxis filter for 3 hours in a 37°C humidified 95% air/5% CO2 incubator. Following the 3 hour migration period, nonmigrating cells on the upper side of the filter were removed with a rubber scraper and migrating cells on the underside of the filter were stained with DiffQuick prior to imaging under a bright field microscope. Images of three 20x fields corresponding to the top left, top right, and bottom center side of each well were taken for each well. The number of cells in each image was counted and an average number of cells per 20X field for each well was determined. Each sample was tested in quadruplicate and the mean number of migrated cells for each of the macrophage-conditioned medias was determined. Each experiment was repeated three times and the results reported represent the combined average for all assays performed.

3.7 Statistical Analysis

Data were analyzed for potential correlations between the histomorphologic scores and in vivo macrophage phenotype using Pearson's correlation coefficient. Results of the Boyden chamber assays were evaluated using a student's T-test. A p-value of $p<0.05$ was considered statistically significant. All analyses were conducted using MATLAB software (MathWorks).

4.0 Results

4.1 Histomorphologic Analysis

Each material elicited a distinct host tissue remodeling response that was characterized by varying degrees of cellular infiltration, vascularization, connective tissue deposition and tissue remodeling. Despite differences in the host tissue response to each material, the responses could be characterized as falling into one of three general qualitative and quantitative groups (Figures 1 and 2). The groups were characterized by chronic inflammation and foreign body response (quantitative score <5; Group 1), early inflammatory cell infiltration with decreased cellularity and little evidence of constructive remodeling at later time points (5< quantitative score <10; Group 2), and early infiltration by inflammatory cells and signs of constructive remodeling at later time points (quantitative score >10; Group 3).

The host tissue remodeling response to materials in Group 1 (Figure 1A) was characterized by little to no cellular infiltration or vasculature within the implant, a dense population of mononuclear macrophages at the host tissue interface, multinucleate giant cells at the periphery of the implant, the deposition of disorganized connective tissues surrounding the implanted test article, and little to no degradation of the material at 14 days. By 35 days, the materials in Group 1 were still largely intact, surrounded by a macrophage and multinucleate giant cell population which was increased in number compared to 14 days, and encapsulated within dense collagenous connective tissue with no evidence of constructive tissue remodeling (i.e. poor connective tissue organization and lack of muscle ingrowth).

The host tissue remodeling response to materials in Group 2 (Figure 1B) was characterized by an initially dense infiltration of mononuclear cells within the mesh, a small degree of device degradation and neo-matrix deposition, and limited vascularization at 14 days. At 35 days the host response to materials in Group 2 was characterized by a distinct decrease in cellularity, both within and surrounding the implanted mesh, limited device degradation, and limited new host tissue deposition. Limited ingrowth of muscle tissue was noted at the periphery of some materials at 35 days. Group 2 was not subject to the multinucleate giant cell and encapsulation type response observed in Group 1.

The host tissue remodeling response to materials in Group 3 (Figure 1C) was characterized by a dense infiltrate of mononuclear cells at early time points, accompanied by deposition of organized connective tissue, the presence of vasculature throughout the materials, and rapid degradation. By 35 days, the original material was not identifiable by histologic evaluation and the remodeling site was composed of organized host connective tissue and islands of skeletal muscle both at the periphery and, to a limited extent, within the center of the

remodeling site. This response was consistent with the early stages of constructive remodeling which have been observed in other studies utilizing similar materials [5, 8]. Examples of the host tissue remodeling response to one of the materials from each group as well as the quantitative score for each of the mesh materials tested are shown in Figures 1 and 2, respectively.

4.2 Macrophage Polarization and Spatial Distribution

The spatial distribution of the macrophages within the implantation site at 14 days could be grouped into three distinct categories, which correspond to the those described above for the histologic response (Figure 3). Materials which resulted in a foreign body response and encapsulation (Group 1, Figure 3A) were characterized by accumulation of macrophages at the periphery of the material with few macrophages observed within the material at 14 days. Macrophages at the interface of the mesh and host tissue in Group 1 were predominantly of the M1 phenotype, and foreign body giant cells were present. A small number of macrophages were occasionally observed infiltrating the periphery of the mesh materials and were predominantly of the M1 phenotype. M2 phenotype macrophages were present within the host tissue of the remodeling site, but were few in number and only observed away from the surface of the material.

Those scaffold materials which resulted in early cellular infiltration but were not encapsulated (Group 2, Figure 3B) were characterized by a dense accumulation of cells both surrounding and within the materials at 14 days. These cells were of a mixed M1 and M2 phenotype. M2 phenotype macrophages were also present at the periphery of the remodeling site and at the interface with the mesh materials. Materials which resulted in early stages of constructive remodeling (Group 3, Figure 3C) were characterized by a dense infiltration of cells both surrounding and within the device materials; a finding which was similar to that observed for Group 2. These cells were of a mixed M1 and M2 phenotype. However, more M2 cells were observed to be present at the interface of the material with host tissue than for Group 2. M2 phenotype macrophages were also present at the periphery of remodeling site and at the interface with the mesh material.

The macrophage response at 35 days was less distinct between groups than at 14 days. Materials in Group 1 were again characterized by an accumulation of primarily M1 macrophages at the surface of the material. Again, few macrophages were observed within the materials, and those that were observed were primarily of an M1 phenotype. Groups 2 and 3 were both characterized by a reduction in the number of macrophages present both at the host tissue interface and throughout the materials. The cells that were present were of a mixed M1/M2 phenotype. Interestingly, in all groups, a population consisting of predominantly M2 macrophages was observed at the periphery of the site of implantation. In Group 1 this corresponded to the area of dense encapsulating connective tissue formation, while in Groups 2 and 3 this corresponded to areas of more organized, site-appropriate tissue formation. It should be noted that cells concurrently expressing markers of both M1 and M2 phenotypes were observed at both 14 and 35 days, but the number and spatial distribution of these cells was not quantified in the present study. Examples of the macrophage response at

14 days as well as quantitative values for each macrophage population within the site of remodeling for each mesh material are shown in Figures 3 and 4, respectively.

Correlation analysis (Pearson) was performed to determine statistically significant relationships between macrophage phenotype and histologic score. Results showed that there were strong, statistically significant correlations between macrophage phenotype at 14 days and the histologic score at 14 days. Both the number of M2 cells and the ratio of M2:M1 cells were found to be strongly correlated with the total histologic score at 14 days (r^2=0.525 and p=0.044, r^2=0.577 and p=0.024, respectively). Neither the number of M0 nor the number of M1 macrophages at 14 days was found to be statistically correlated with the histologic score at 14 days. It was shown that there were no statistically significant correlations between macrophage phenotype at 35 days and the histologic score at 35 days. However, both the number of M2 macrophages and the ratio of M2:M1 macrophages within the remodeling site at 14 days were found to be correlated with the histologic score at 35 days (r^2=0.686 and p=0.005, r^2=0.686 and p=0.005, respectively), suggesting that macrophage phenotype at early time points is a statistically significant predictor of histologic outcome at later time points. Analysis correlating macrophage phenotype and specific aspects of the remodeling response (i.e. cellularity, muscle ingrowth, encapsulation, etc.) at both 14 and 35 days was performed and statistically significant relationships were identified. The results of this analysis are provided in Supplemental Table 2.

4.3 Chemotaxis of Myoblast-like cells to M0, M1, and M2 Macrophage Conditioned Media

Results showed that C2C12 myoblast-like cell migration was similar for media from cultures of all macrophage types harvested at 4 hours. Results from medias harvested at 8, 12, and 24 hours show that both M0 and M2 conditioned medias caused greater myoblast migration than did M1 conditioned media. However, all media types were observed to cause migration which was greater than or equal to that of the positive control at 8 hours. M1 conditioned media caused migration which was less than the positive control at 12 and 24 hours. The greatest migration response was seen in 8 hour conditioned medias from M0 and M2 cells. No significant differences were found between M0 and M2 conditioned medias at any time point. Differences were found for the M0 and M2 groups as compared to the M1 medias harvested at 8, 12, and 24 hours. The results of the Boyden chamber assay are shown in Figure 5.

5.0 Discussion

The present study investigated the host response to 14 commercially available biologic surgical mesh materials and showed that macrophage phenotype at 14 days post implantation is correlated with both the early histomorphologic response and the later tissue remodeling outcome. Each material was distinct in its source tissue and methods of preparation and elicited a response that was characterized by a distinct histomorphologic progression of tissue remodeling at 14 and 35 days which is similar to that reported in preclinical and clinical studies [8, 23–29]. In addition, the M2 phenotype that was associated with the most constructive tissue remodeling was also shown to secrete products that are chemotactic for C2C12 myoblasts; a skeletal muscle progenitor-like cell type. Despite the observed differences in the histomorphologic appearance of the remodeling site at 35 days,

all materials elicited a morphologically similar population of mononuclear cells at 14 days when examined with routine stains such as H&E or Masson's trichrome. This mononuclear cell response is typically characterized as chronic inflammation with associated negative implications for downstream tissue remodeling. However, as the results of the present study show, the downstream outcome is not necessarily granulation tissue, a foreign body response, or the deposition of dense scar tissue within the site of remodeling. These disparate outcomes suggest that, although the majority of the cells present in the early stages of remodeling may be morphologically similar, critical phenotypic differences can exist that have marked effects upon the outcome. These phenotypic differences are likely dependent upon some aspect of the implanted material such as surface topology, available ligands, and/or degradability.

The results of the present study show that phenotypic differences in macrophages are indeed associated with distinct tissue remodeling outcomes. Although cause-effect relationships were not proven, increases in the M2 macrophage population and a greater ratio of M2:M1 cells within the site of tissue remodeling at 14 days were very clearly associated with higher, more favorable histologic scores and were predictive of a more desirable remodeling outcome at 35 days. These findings suggest that the phenotypic profile of the macrophages participating in the host response at early time points can be used to make quantitative predictions of downstream tissue remodeling outcomes for surgical mesh materials composed of naturally occurring biomaterials.

The exact mechanisms by which macrophages influence tissue remodeling outcomes remain largely unknown or at least unproven. In vitro work performed in the present studies showed that the culture supernatants from all macrophage populations (M0, M1, and M2) were capable of promoting the chemotaxis of a muscle specific progenitor-like cell population (C2C12). However, the degree of chemotaxis was shown to differ depending on the polarization profile of the macrophage population investigated. M0 and M2 macrophages were shown to promote greater chemotaxis than did M1 cells. These results parallel those in another in vitro study which investigated the ability of M1 and M2 macrophages to recruit vessel associated progenitor cell populations [30]. The study showed that both M1 and M2 polarized macrophages were capable of inducing chemotaxis of progenitor-like cells. However, the number and phenotype of the cells and the pathways by which they were recruited were shown to be distinct for M1 and M2 cells.

Additional studies have shown that M1 and M2 macrophages have distinct effects upon the phenotype and survival of recruited cells [21, 31]. One such study showed that neuronal cells which were exposed to media conditioned by M1 macrophages exhibited a decrease in viability as well as a decrease in neurite length, while those cells exposed to media conditioned by M2 macrophages showed improved survival and a greater degree of neurite extension [21]. Comparable results have been reported for muscle cells, showing that M1 macrophages cause cell lysis while M2 macrophages support satellite cell proliferation and muscle regeneration [31]. These results suggest that polarization towards the M2 phenotype generally promotes a positive tissue remodeling environment via attenuation of the pro-inflammatory M1 population and the host T-cell response as well as through beneficial paracrine effects upon tissue specific cell populations. Dysregulation and excessive long-

term polarization of the M1/M2 phenotypic profile towards either an M1 or an M2 extreme, however, may have negative effects upon the tissue remodeling outcome.

It has been shown that macrophages may also be capable of affecting tissue remodeling through more direct, non-paracrine mechanisms, suggesting a previously unrecognized role for macrophages in the tissue remodeling process [32–36]. A recent study showed that bioactive molecules obtained from the degradation of a material similar to the Matristem mesh used in the present study promoted the recruitment of multi-potential progenitor cells to sites of tissue injury when used in a model of mammalian digit amputation [32]. The recruited cells concurrently expressed markers of multipotency (Sox2, Sca1 and Rex1) and markers suggestive of an activated macrophage phenotype (CD68). Further investigation showed that it was possible to differentiate these cells along all three germ cell lineages suggesting a potentially unique role for cells possessing the CD68 marker in biologic mesh remodeling. Other studies have suggested that macrophages share characteristics with progenitor cells and are capable of myeloid to mesenchymal transition during the response to implanted materials, again suggesting previously unrecognized roles for mononuclear cells with macrophage appearance and possessing surface markers characteristic of macrophage activation in the response to implanted materials [33, 34, 36].

The exact mechanisms by which certain biologic mesh materials are capable of modulating the host macrophage population towards a more constructive remodeling phenotype are not fully understood; however, it has been shown that the presence of large amounts of cellular material and chemical cross-linking have detrimental effects upon this ability [6–8, 37]. This response is not surprising in the case of xenogeneic cellular components, such as the α-Gal epitope, which may be recognized by the host immune system and elicit an immune response following implantation [38, 39]. Other molecules, including those associated with cell death, are also known to have potent immunomodulatory effects [40, 41]. These cell death associated molecules, collectively termed damage associated molecular pattern molecules (DAMPs), are recognized by pattern recognition receptors on cells of the innate immune system. Therefore, large amounts of these molecules within biologic materials that derive from mammalian tissues as a result of inefficient removal during processing or due to cellular death upon implantation may have detrimental effects upon the ability of ECM scaffold materials to promote constructive tissue remodeling. Virtually all biologic materials are derived from mammalian tissues and contain remnants of cellular debris; however the threshold amount and specific effector molecules which are responsible for determining M1 versus M2 phenotype remain unknown [42]. Additionally, endotoxin is a ubiquitous contaminant of surgical mesh materials which can have potentially detrimental effects upon the host response following implantation. Endotoxin levels of the materials used in the present study were assumed to be below the FDA mandated threshold for biologic devices. However, as is shown in the present study, modulation of the host macrophage response towards a more pro-inflammatory, M1, type response by contaminants such as endotoxin may result in less desirable outcomes.

Chemical cross-linking of biologic mesh materials following decellularization changes both the ultrastructure and, to a smaller degree, the composition and surface topology of the material [43]. Therefore, it is logical to assume that interactions between the surface of the

material and the cells which participate in the host response are important determinants of the downstream tissue remodeling outcome. Alternatively, inability of the material to degrade may prevent the release of the bioactive matricryptic peptides contained within the components of the ECM that have been shown to have potent antibacterial, chemotactic, and mitogenic properties [44–50]. All of the chemically crosslinked materials investigated in the present study (Avaulta Plus, Collamend, PelviSoft) resulted in a chronic foreign body response and downstream encapsulation. Additionally, in the present study, non-crosslinked mesh materials derived from dermis (AlloMax, AlloDerm, FlexHD, InteXen, Strattice Firm, Strattice Pliable, Surgimend, XenForm) degraded more slowly than materials derived from sources such as small intestine and urinary bladder. Differences in the histomorphologic response following implantation may be due, at least in part, to slower release of potentially beneficial bioactive peptides contained within the scaffold material. Indeed, a number of matricryptic peptides have been shown to signal through pattern recognition receptors and scavenger receptors, both of which play an important role in macrophage polarization and behavior [51–53]. Further work is required, however, to determine the role, if any, played by these molecules in the observed differences in macrophage phenotype in the present and previous studies.

There were several limitations in the present study. Only three surface markers (CD68, CCR7, and CD206) were utilized for characterization of the M1/M2 profile of the macrophages participating in the host response. These markers were chosen both because they are known to be highly indicative of M1 (CCR7) or M2 (CD206) polarization in multiple animal and human models and because of the nature of the triple staining performed [10, 54]. That is, three individual antibodies, each made in a separate species, were required. It should be noted that one of these markers, CCR7, is also known to be expressed by certain subsets of dendritic and T-cell populations. Both of these cell types are known to participate in ECM remodeling [55–57], albeit in much smaller numbers than macrophages [6, 7, 37]. The present study did not attempt to distinguish CCR7+ macrophages, dendritic cells, and T-cells. It should also be noted that macrophage polarization occurs on a spectrum between M1 and M2 and markers for all intermediate macrophage phenotypes have not been well established, especially in the context of the response to biomaterials. Further, while observed, no attempt was made in the present study to quantify the number of cells expressing both M1 and M2 markers concurrently. The role of such cells expressing intermediate markers of M1 and M2 phenotypes is unknown in the context of tissue remodeling and biomaterials. Future studies should include more extensive characterization of macrophage phenotype at various stages of the remodeling process. Assays for more fully characterizing macrophage phenotype may include flow cytometry, analysis of cytokine profiles (mRNA and protein), and depletion of specific macrophage subtypes during the remodeling process. These assays may provide a more in-depth and potentially mechanistic understanding of the role of macrophages in tissue remodeling following the implantation of a biomaterial. The present study also utilized immortalized macrophage and myoblast-like cell lines. While the behavior of these cell lines is well known and has been characterized in a large number of studies, it remains unknown if the exact behavior observed in the present study can be extrapolated to primary cells or if similar phenomenon exist in vivo.

In the present study, a population of CD68+ macrophages was observed, some of which did not stain positive for either M1 or M2 surface markers. These cells may have only just arrived at the site of remodeling and, thus, might not yet have been stimulated to undergo polarization towards an M1 or M2 phenotype. Similarly, cells expressing various combinations of CD68, CCR7 and CD206 were observed, but not quantified. It is possible that a percentage of the macrophages participating in the host response to ECM scaffolds may express intermediate or previously unrecognized phenotypes.

6.0 Conclusion

The histomorphologic progression of remodeling associated with each of the implanted materials examined in the present study is similar to that reported clinically for each of the devices examined. The present study clearly shows that there is a strong correlation between the early macrophage response to implanted ECM scaffold materials and the outcome of tissue remodeling. Further, the results of the present study suggest that downstream effects may be due to the recruitment and survival of different cell populations to the sites of remodeling associated with materials that elicit an M1 versus M2 response. A more thorough understanding of these factors which underlie the patterns of macrophage polarization observed in the present study will logically influence the design of next generation biomaterials and the development of regenerative medicine strategies for the formation of new functional host tissues as opposed to inflammation and scarring.

Supplementary Material

Refer to Web version on PubMed Central for supplementary material.

Acknowledgments

Funding for this study was provided through a grant from the National Institutes of Health (R01 AR054940-01). Additionally, Bryan Brown was supported by NIH fellowship F31 EB007914.

8.0 References

1. Badylak SF. The extracellular matrix as a biologic scaffold material. Biomaterials. 2007 Sep; 28(25):3587–3593. [PubMed: 17524477]
2. Badylak SF. Xenogeneic extracellular matrix as a scaffold for tissue reconstruction. Transpl Immunol. 2004 Apr; 12(3–4):367–377. [PubMed: 15157928]
3. Badylak SF, Brown BN, Gilbert TW, Daly KA, Huber A, Turner NJ. Biologic scaffolds for constructive tissue remodeling. Biomaterials. 2011 Jan; 32(1):316–319. [PubMed: 21125721]
4. Turner NJ, Yates AJ Jr, Weber DJ, Qureshi IR, Stolz DB, Gilbert TW, et al. Xenogeneic extracellular matrix as an inductive scaffold for regeneration of a functioning musculotendinous junction. Tissue Eng Part A. 2010 Nov; 16(11):3309–3317. [PubMed: 20528669]
5. Valentin JE, Turner NJ, Gilbert TW, Badylak SF. Functional skeletal muscle formation with a biologic scaffold. Biomaterials. 2010 Oct; 31(29):7475–7484. [PubMed: 20638716]
6. Brown BN, Valentin JE, Stewart-Akers AM, McCabe GP, Badylak SF. Macrophage phenotype and remodeling outcomes in response to biologic scaffolds with and Without a cellular component. Biomaterials. 2009 Mar; 30(8):1482–1491. [PubMed: 19121538]
7. Badylak SF, Valentin JE, Ravindra AK, McCabe GP, Stewart-Akers AM. Macrophage phenotype as a determinant of biologic scaffold remodeling. Tissue Eng Part A. 2008 Nov; 14(11):1835–1842. [PubMed: 18950271]

8. Valentin JE, Badylak JS, McCabe GP, Badylak SF. Extracellular matrix bioscaffolds for orthopaedic applications. A comparative histologic study. J Bone Joint Surg Am. 2006 Dec; 88(12): 2673–2686. [PubMed: 17142418]

9. Gordon S, Taylor PR. Monocyte and macrophage heterogeneity. Nat Rev Immunol. 2005 Dec; 5(12):953–964. [PubMed: 16322748]

10. Mantovani A, Sica A, Sozzani S, Allavena P, Vecchi A, Locati M. The chemokine system in diverse forms of macrophage activation and polarization. Trends Immunol. 2004 Dec; 25(12):677–686. [PubMed: 15530839]

11. Stout RD, Watkins SK, Suttles J. Functional plasticity of macrophages: in situ reprogramming of tumor-associated macrophages. J Leukoc Biol. 2009 Nov; 86(5):1105–1109. [PubMed: 19605698]

12. Stout RD, Suttles J. Functional plasticity of macrophages: reversible adaptation to changing microenvironments. J Leukoc Biol. 2004 Sep; 76(3):509–513. [PubMed: 15218057]

13. Adamson R. Role of macrophages in normal wound healing: an overview. J Wound Care. 2009 Aug; 18(8):349–351. [PubMed: 19862875]

14. Anderson, JM. Inflammation, Wound Healing, and the Foreign Body Response. In: Ratner, BD.; Hoffman, AS.; Schoen, FJ.; Lemons, JE., editors. Biomaterials Science: An Introduction to Materials in Medicine. San Diego, CA: Elsivier; 2004. p. 296-304.

15. Mills CD, Kincaid K, Alt JM, Heilman MJ, Hill AM. M-1/M-2 macrophages and the Th1/Th2 paradigm. J Immunol. 2000 Jun 15; 164(12):6166–6173. [PubMed: 10843666]

16. Mosser DM. The many faces of macrophage activation. J Leukoc Biol. 2003 Feb; 73(2):209–212. [PubMed: 12554797]

17. Shimada K. Immune system and atherosclerotic disease: heterogeneity of leukocyte subsets participating in the pathogenesis of atherosclerosis. Circ J. 2009 Jun; 73(6):994–1001. [PubMed: 19430164]

18. Allavena P, Sica A, Garlanda C, Mantovani A. The Yin-Yang of tumor-associated macrophages in neoplastic progression and immune surveillance. Immunol Rev. 2008 Apr.222:155–161. [PubMed: 18364000]

19. Fuentes L, Roszer T, Ricote M. Inflammatory mediators and insulin resistance in obesity: role of nuclear receptor signaling in macrophages. Mediators Inflamm. 2010; 2010:219583. [PubMed: 20508742]

20. Deonarine K, Panelli MC, Stashower ME, Jin P, Smith K, Slade HB, et al. Gene expression profiling of cutaneous wound healing. J Transl Med. 2007; 5:11. [PubMed: 17313672]

21. Kigerl KA, Gensel JC, Ankeny DP, Alexander JK, Donnelly DJ, Popovich PG. Identification of two distinct macrophage subsets with divergent effects causing either neurotoxicity or regeneration in the injured mouse spinal cord. J Neurosci. 2009 Oct 28; 29(43):13435–13444. [PubMed: 19864556]

22. Badylak S, Kokini K, Tullius B, Simmons-Byrd A, Morff R. Morphologic study of small intestinal submucosa as a body wall repair device. J Surg Res. 2002 Apr; 103(2):190–202. [PubMed: 11922734]

23. de Castro Bras LE, Shurey S, Sibbons PD. Evaluation of crosslinked and non-crosslinked biologic prostheses for abdominal hernia repair. Hernia. 2011 Jul 31.

24. Deeken CR, Melman L, Jenkins ED, Greco SC, Frisella MM, Matthews BD. Histologic and biomechanical evaluation of crosslinked and non-crosslinked biologic meshes in a porcine model of ventral incisional hernia repair. J Am Coll Surg. 2011 May; 212(5):880–888. [PubMed: 21435917]

25. Melman L, Jenkins ED, Hamilton NA, Bender LC, Brodt MD, Deeken CR, et al. Early biocompatibility of crosslinked and non-crosslinked biologic meshes in a porcine model of ventral hernia repair. Hernia. 2011 Apr; 15(2):157–164. [PubMed: 21222009]

26. Connor J, McQuillan D, Sandor M, Wan H, Lombardi J, Bachrach N, et al. Retention of structural and biochemical integrity in a biological mesh supports tissue remodeling in a primate abdominal wall model. Regen Med. 2009 Mar; 4(2):185–195. [PubMed: 19317639]

27. Sandor M, Xu H, Connor J, Lombardi J, Harper JR, Silverman RP, et al. Host response to implanted porcine-derived biologic materials in a primate model of abdominal wall repair. Tissue Eng Part A. 2008 Dec; 14(12):2021–2031. [PubMed: 18657025]

28. Hodde J, Hiles M. Constructive soft tissue remodelling with a biologic extracellular matrix graft: overview and review of the clinical literature. Acta Chir Belg. 2007 Nov-Dec;107(6):641–647. [PubMed: 18274177]
29. Rice RD, Ayubi FS, Shaub ZJ, Parker DM, Armstrong PJ, Tsai JW. Comparison of Surgisis, AlloDerm, and Vicryl Woven Mesh grafts for abdominal wall defect repair in an animal model. Aesthetic Plast Surg. 2010 Jun; 34(3):290–296. [PubMed: 19967358]
30. Lolmede K, Campana L, Vezzoli M, Bosurgi L, Tonlorenzi R, Clementi E, et al. Inflammatory and alternatively activated human macrophages attract vessel-associated stem cells, relying on separate HMGB1- and MMP-9-dependent pathways. J Leukoc Biol. 2009 May; 85(5):779–787. [PubMed: 19197071]
31. Villalta SA, Rinaldi C, Deng B, Liu G, Fedor B, Tidball JG. Interleukin-10 reduces the pathology of mdx muscular dystrophy by deactivating M1 macrophages and modulating macrophage phenotype. Hum Mol Genet. 2011 Feb 15; 20(4):790–805. [PubMed: 21118895]
32. Agrawal V, Johnson SA, Reing J, Zhang L, Tottey S, Wang G, et al. Epimorphic regeneration approach to tissue replacement in adult mammals. Proc Natl Acad Sci U S A. 2010 Feb 23; 107(8):3351–3355. [PubMed: 19966310]
33. Mooney JE, Rolfe BE, Osborne GW, Sester DP, van Rooijen N, Campbell GR, et al. Cellular plasticity of inflammatory myeloid cells in the peritoneal foreign body response. Am J Pathol. 2010 Jan; 176(1):369–380. [PubMed: 20008135]
34. Le SJ, Gongora M, Zhang B, Grimmond S, Campbell GR, Campbell JH, et al. Gene expression profile of the fibrotic response in the peritoneal cavity. Differentiation. 2010 Apr-Jun;79(4–5): 232–243. [PubMed: 20395036]
35. Madden LR, Mortisen DJ, Sussman EM, Dupras SK, Fugate JA, Cuy JL, et al. Proangiogenic scaffolds as functional templates for cardiac tissue engineering. Proc Natl Acad Sci U S A. 2010 Aug 24; 107(34):15211–15216. [PubMed: 20696917]
36. Charriere GM, Cousin B, Arnaud E, Saillan-Barreau C, Andre M, Massoudi A, et al. Macrophage characteristics of stem cells revealed by transcriptome profiling. Exp Cell Res. 2006 Oct 15; 312(17):3205–3214. [PubMed: 16934250]
37. Valentin JE, Stewart-Akers AM, Gilbert TW, Badylak SF. Macrophage participation in the degradation and remodeling of extracellular matrix scaffolds. Tissue Eng Part A. 2009 Jul; 15(7): 1687–1694. [PubMed: 19125644]
38. Cooper DK, Good AH, Koren E, Oriol R, Malcolm AJ, Ippolito RM, et al. Identification of alpha-galactosyl and other carbohydrate epitopes that are bound by human anti-pig antibodies: relevance to discordant xenografting in man. Transpl Immunol. 1993; 1(3):198–205. [PubMed: 7521740]
39. Galili U, Macher BA, Buehler J, Shohet SB. Human natural anti-alpha-galactosyl IgG. II. The specific recognition of alpha (1----3)-linked galactose residues. J Exp Med. 1985 Aug 1; 162(2): 573–582. [PubMed: 2410529]
40. Chen GY, Nunez G. Sterile inflammation: sensing and reacting to damage. Nature reviews. 2010 Nov 19.
41. Lotze MT, Zeh HJ, Rubartelli A, Sparvero LJ, Amoscato AA, Washburn NR, et al. The grateful dead: damage-associated molecular pattern molecules and reduction/oxidation regulate immunity. Immunol Rev. 2007 Dec.220:60–81. [PubMed: 17979840]
42. Gilbert TW, Freund JM, Badylak SF. Quantification of DNA in biologic scaffold materials. J Surg Res. 2009 Mar; 152(1):135–139. [PubMed: 18619621]
43. Brown BN, Barnes CA, Kasick RT, Michel R, Gilbert TW, Beer-Stolz D, et al. Surface characterization of extracellular matrix scaffolds. Biomaterials. 2010 Jan; 31(3):428–437. [PubMed: 19828192]
44. Brennan EP, Tang XH, Stewart-Akers AM, Gudas LJ, Badylak SF. Chemoattractant activity of degradation products of fetal and adult skin extracellular matrix for keratinocyte progenitor cells. J Tissue Eng Regen Med. 2008 Dec; 2(8):491–498. [PubMed: 18956412]
45. Brennan EP, Reing J, Chew D, Myers-Irvin JM, Young EJ, Badylak SF. Antibacterial activity within degradation products of biological scaffolds composed of extracellular matrix. Tissue Eng. 2006 Oct; 12(10):2949–2955. [PubMed: 17518662]

46. Haviv F, Bradley MF, Kalvin DM, Schneider AJ, Davidson DJ, Majest SM, et al. Thrombospondin-1 mimetic peptide inhibitors of angiogenesis and tumor growth: design, synthesis, and optimization of pharmacokinetics and biological activities. J Med Chem. 2005 Apr 21; 48(8):2838–2846. [PubMed: 15828822]
47. Li F, Li W, Johnson S, Ingram D, Yoder M, Badylak S. Low-molecular weight peptides derived from extracellular matrix as chemoattractants for primary endothelial cells. Endothelium. 2004 May-Aug;11(3–4):199–206. [PubMed: 15370297]
48. Sarikaya A, Record R, Wu CC, Tullius B, Badylak S, Ladisch M. Antimicrobial activity associated with extracellular matrices. Tissue Eng. 2002 Feb; 8(1):63–71. [PubMed: 11886655]
49. Reing JE, Zhang L, Myers-Irvin J, Cordero KE, Freytes DO, Heber-Katz E, et al. Degradation products of extracelluar matrix affect cell migration and proliferation. Tissue Eng Part A. 2009 Mar; 15(3):605–614. [PubMed: 18652541]
50. Vorotnikova E, McIntosh D, Dewilde A, Zhang J, Reing JE, Zhang L, et al. Extracellular matrix-derived products modulate endothelial and progenitor cell migration and proliferation in vitro and stimulate regenerative healing in vivo. Matrix Biol. 2010 Oct; 29(8):690–700. [PubMed: 20797438]
51. Davis GE. Matricryptic sites control tissue injury responses in the cardiovascular system: relationships to pattern recognition receptor regulated events. J Mol Cell Cardiol. 2010 Mar; 48(3): 454–460. [PubMed: 19751741]
52. Pluddemann A, Neyen C, Gordon S. Macrophage scavenger receptors and host-derived ligands. Methods. 2007 Nov; 43(3):207–217. [PubMed: 17920517]
53. Adair-Kirk TL, Senior RM. Fragments of extracellular matrix as mediators of inflammation. Int J Biochem Cell Biol. 2008; 40(6–7):1101–1110. [PubMed: 18243041]
54. Martinez FO, Gordon S, Locati M, Mantovani A. Transcriptional profiling of the human monocyte-to-macrophage differentiation and polarization: new molecules and patterns of gene expression. J Immunol. 2006 Nov 15; 177(10):7303–7311. [PubMed: 17082649]
55. Badylak SF, Gilbert TW. Immune response to biologic scaffold materials. Semin Immunol. 2008 Apr; 20(2):109–116. [PubMed: 18083531]
56. Palmer EM, Beilfuss BA, Nagai T, Semnani RT, Badylak SF, van Seventer GA. Human helper T cell activation and differentiation is suppressed by porcine small intestinal submucosa. Tissue Eng. 2002 Oct; 8(5):893–900. [PubMed: 12459068]
57. Allman AJ, McPherson TB, Merrill LC, Badylak SF, Metzger DW. The Th2-restricted immune response to xenogeneic small intestinal submucosa does not influence systemic protective immunity to viral and bacterial pathogens. Tissue Eng. 2002 Feb; 8(1):53–62. [PubMed: 11886654]

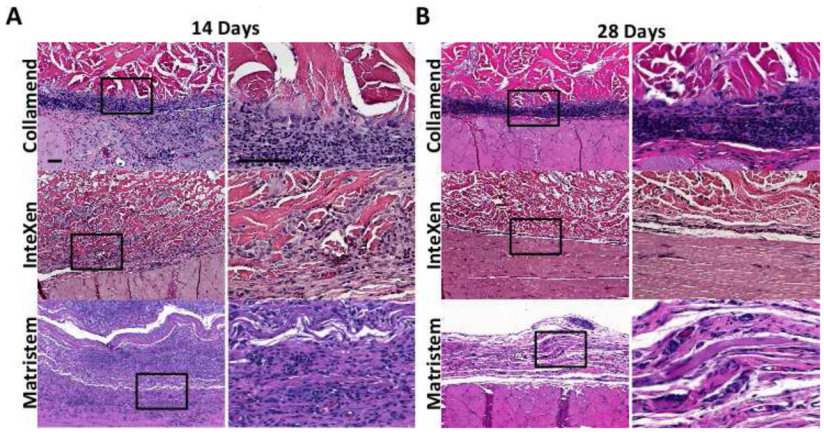

Figure 1.

Photomicrographs of hematoxylin and eosin stained slides showing examples of the host remodeling response to test articles in Group 1 (Collamend), Group 2 (InteXen) and Group 3 (MatriStem) at 14 (A) and 35 days (B). Scale bars = 100 μm. Images with higher magnification represent the area within the black box in lower magnification images.

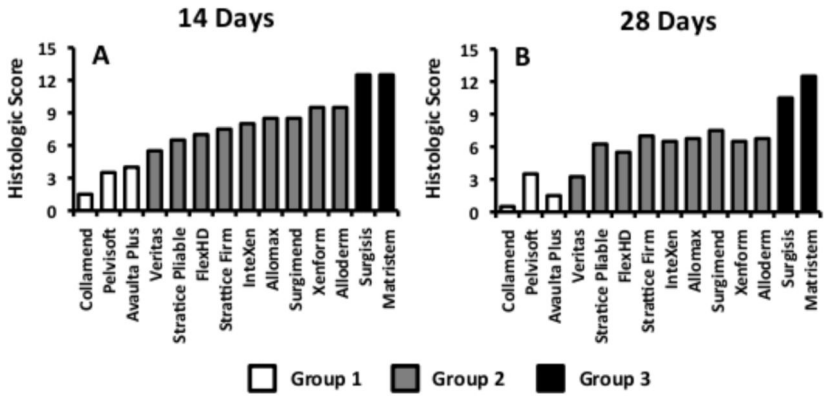

Figure 2.

Quantitative histologic scores at 14 days (A) and 35 days (B) post-implantation. Data are presented as the mean for each sample type (n=2). White bars represent materials from Group 1, grey bars represent materials from Group 2, and black bars represent materials from Group 3. Higher scores are more indicative of a constructive remodeling response while low scores are more indicative of a scar tissue or foreign body type response.

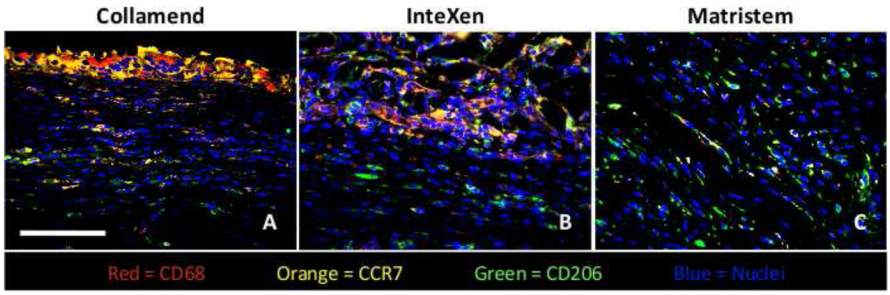

Figure 3.

Immunofluorescent images showing examples of the host macrophage response to mesh materials from Group 1 (Collamend, A), Group 2 (InteXen, B) and Group 3 (MatriStem, C) at 14 days post implantation. Scale bar = 100 μm. CD68 (pan-macrophage) = red, CCR7 (M1) = orange, CD206 (M2) = green, DRAQ5 (nuclei) = blue.

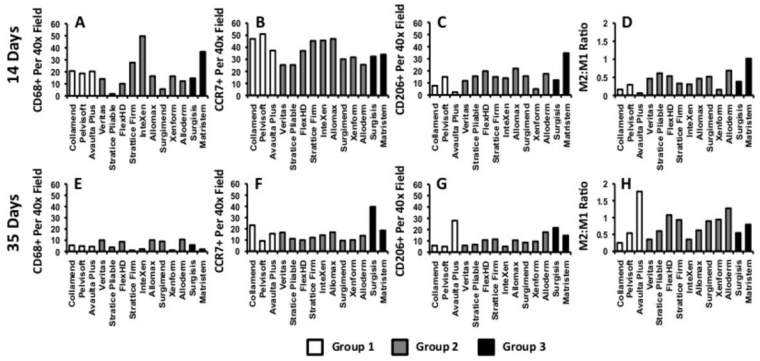

Figure 4.

Average number of macrophages expressing markers indicative of M0, (A,E), M1 (B,F) and M2 (C,G) polarization per high power microscope field as well as the ratio of M2:M1 marker expressing cells (D,H) at 14 days (A–D) and 35 days (E–H). Quantitative results presented as the mean for each sample type (n=2). White bars represent materials from Group 1, grey bars represent materials from Group 2, and black bars represent materials from Group 3.

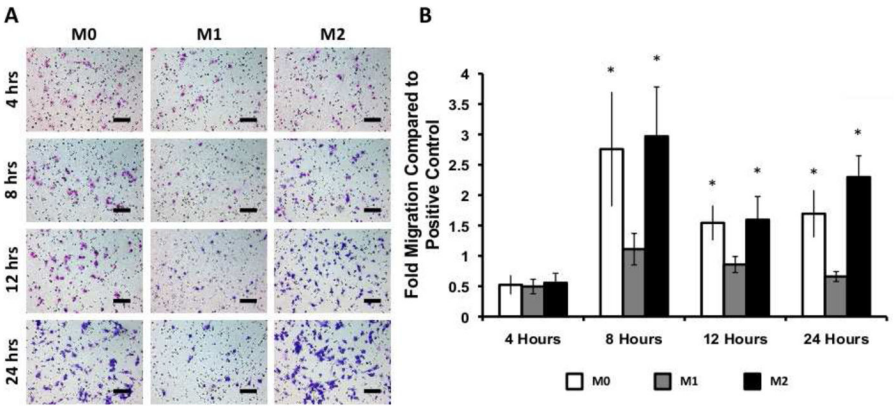

Figure 5.

Photomicrographs showing representative Boyden chamber assay results obtained using M0, M1, and M2 macrophage conditioned media (A). Quantification of C2C12 myoblast migration towards culture supernatants from M0, M1, and M2 macrophages at 4, 8, 12, and 24 hours post-implantation (B). White bar represents migration towards M0 supernatants, grey bar represents migration towards M1 supernatants, and black bar represents migration towards M2 supernatants. Scale bar = 100 μm. * denotes significance as compared to M1 with $p<0.05$.

Table 1

Name, manufacturer and composition of the biologically derived surgical mesh materials examined.

Test Article	Manufacturer	Composition
AlloMax	C. R. BARD, Inc.	Human dermis
AlloDerm	LifeCell Corporation	Human dermis
Avaulta Plus	C. R. BARD, Inc.	Porcine dermis (crosslinked)
CollaMend	C. R. BARD, Inc.	Porcine dermis (crosslinked)
Flex HD	Ethicon, Inc.	Human dermis
InteXen LP	American Medical Systems	Porcine dermis
MatriStem	Acell, Inc.	Porcine urinary bladder (4 layer)
PelviSoft	C. R. BARD, Inc.	Porcine dermis (crosslinked)
Strattice Firm	LifeCell Corporation	Porcine dermis
Strattice Pliable	LifeCell Corporation	Porcine dermis
Sugisis	Cook Medical	Porcine small intestinal submucosa (8 layer)
SurgiMend	TEI Biosciences, Inc.	Fetal bovine dermis
Veritas	Synovis Life Technologies, Inc.	Bovine pericardium
Xenform	Boston Scientific Corporation	Fetal bovine dermis

Table 2

Quantitative histologic scoring criteria at 14 and 35 days. A description of each category is shown. Higher scores are more indicative of a constructive remodeling response while low scores are more indicative of a scar tissue or foreign body type response.

14 Days				
	0	**1**	**2**	**3**
Cellular Infiltration	0 cells per 40X field	1–75 cells per 40X field	75–150 cells per 40x field	more than 150 cells per 40x field
Multinucleated Giant Cells	more than 5 per 40x field	2–5 per 40x field	1 per 40x field	0 per 40x field
Vascularity	0–1 per 40x field	2–5 per 40x field original scaffold disrupted,	6–10 per 40x field	more than 10 per 40x field
		poorly organized new ECM	moderately organized	dense, highly organized
Connective Tissue Organization	original scaffold intact	present	connective tissue present	connective tissue present
Encapsulation	dense tissue encapsulation	moderate encapsulation	slight encapsulation	no encapsulation
Degradation	no degradation	mostly present	some scaffold present	no scaffold present

35 Days				
	0	**1**	**2**	**3**
Multinucleated Giant Cells	more than 5 per 40x field	2–5 per 40x field original scaffold disrupted,	1 per 40x field	0 per 40x field
		poorly organized new ECM	moderately organized	dense, highly organized
Connective Tissue Organization	original scaffold intact	present	connective tissue present	connective tissue present
Muscle Ingrowth	no muscle ingrowth	muscle cells present at periphery	muscle cells present in center	organized muscle present
Encapsulation	dense tissue encapsulation	moderate encapsulation	slight encapsulation	no encapsulation
Degradation	no degradation	mostly present	some scaffold present	no scaffold present